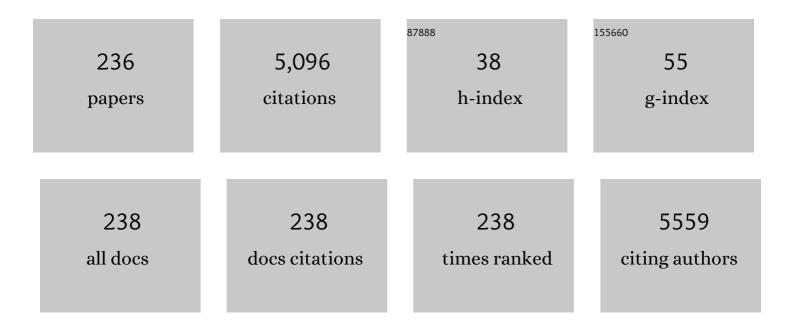
## Kongjun Zhu

List of Publications by Year in descending order

Source: https://exaly.com/author-pdf/7566213/publications.pdf Version: 2024-02-01



Комсили 7ни

#	Article	IF	CITATIONS
1	Optimisation of conductivity of PEO/PVDF-based solid polymer electrolytes in all-solid-state Li-ion batteries. Materials Technology, 2022, 37, 240-247.	3.0	19
2	Enhanced breakdown strength and energy density of multilayered P(VDF-HFP)/Nd-doped BaTiO3 nanofibers composites. Chemical Engineering Journal, 2022, 427, 131811.	12.7	15
3	LiF-Assisted Synthesis of Perovskite-Type Li0.35La0.55TiO3 Solid Electrolyte for Rechargeable Lithium-Metal Batteries. Journal of Electronic Materials, 2022, 51, 736-744.	2.2	5
4	3D poly(vinylidene fluoride–hexafluoropropylen) nanofiber-reinforced PEO-based composite polymer electrolyte for high-voltage lithium metal batteries. Electrochimica Acta, 2022, 404, 139769.	5.2	16
5	Semiconducting BaTiO3@C core-shell structure for improving piezo-photocatalytic performance. Nano Energy, 2022, 93, 106831.	16.0	64
6	Synergic Enhancement of Energy Storage Density and Efficiency in MnO <sub>2</sub> -Doped AgNbO <sub>3</sub> @SiO <sub>2</sub> Ceramics via A/B-Site Substitutions. ACS Applied Materials & Interfaces, 2022, 14, 7052-7062.	8.0	29
7	Ultrahigh reversible lithium storage of hierarchical porous Co–Mo oxides <i>via</i> graphene encapsulation and hydrothermal S-doping. Journal of Materials Chemistry A, 2022, 10, 5373-5380.	10.3	9
8	Constructing Z-scheme structure by loading BiOBr with (010) exposure on the surface of MoS2 and its enhanced photocatalytic property for degrading RhB. Journal of Materials Science: Materials in Electronics, 2022, 33, 6722-6733.	2.2	6
9	Hot pressing process ameliorates internal defects of PBZ/PVDF composite film for a high electrocaloric effect near room temperature. Functional Materials Letters, 2022, 15, .	1.2	2
10	Flexible and Self-Standing Urchinlike V <sub>2</sub> O <sub>3</sub> @Carbon Nanofibers toward Ultralong Cycle Lifespan Lithium-Ion Batteries. ACS Applied Energy Materials, 2022, 5, 3242-3251.	5.1	14
11	Fabrication, Characterization and Drainage Capacity of Single-Channel Porous Alumina Ceramic Membrane Tube. Membranes, 2022, 12, 390.	3.0	3
12	Enhanced energy storage performance of poly(vinylidene fluoride)-based polymer blends via post-treatments. Polymers and Polymer Composites, 2022, 30, 096739112210997.	1.9	2
13	Heterogeneous interface-boosted zinc storage of H2V3O8 nanowire/Ti3C2Tx MXene composite toward high-rate and long cycle lifespan aqueous zinc-ion batteries. Energy Storage Materials, 2022, 50, 63-74.	18.0	37
14	Synthesis of heterostructured dual metal sulfides by a high-temperature mixing hydrothermal method as an ultra-high rate anode for Li-ion batteries. CrystEngComm, 2022, 24, 4698-4704.	2.6	4
15	Effect of Different Ca2+ and Zr4+ Contents on Microstructure and Electrical Properties of (Ba,Ca)(Zr,Ti)O3 Lead-Free Piezoelectric Ceramics. Crystals, 2022, 12, 896.	2.2	3
16	High piezoelectricity in PFN–PNN–PZT quaternary ceramics achieved via composition optimization near morphotropic phase boundary. Ceramics International, 2022, 48, 30891-30899.	4.8	4
17	Enhanced visible-light photocatalytic performances of ZnO through loading AgI and coupling piezo-photocatalysis. Journal of Alloys and Compounds, 2021, 852, 156848.	5.5	39
18	Hydrothermal Synthesis of Various Shape-Controlled Europium Hydroxides. Nanomaterials, 2021, 11, 529.	4.1	8

#	Article	IF	CITATIONS
19	Double-Layered Multifunctional Composite Electrolytes for High-Voltage Solid-State Lithium-Metal Batteries. ACS Applied Materials & Interfaces, 2021, 13, 11958-11967.	8.0	41
20	The electrocaloric effect of PBZ/PVDF flexible composite film near room temperature. Journal of Materials Science: Materials in Electronics, 2021, 32, 12001-12016.	2.2	4
21	Controlled Hydrothermal/Solvothermal Synthesis of Highâ€Performance LiFePO <sub>4</sub> for Liâ€lon Batteries. Small Methods, 2021, 5, e2100193.	8.6	52
22	Preparation of Silicon Hydroxyapatite Nanopowders under Microwave-Assisted Hydrothermal Method. Nanomaterials, 2021, 11, 1548.	4.1	8
23	Zero Lithium Miscibility Gap Enables High-Rate Equimolar Li(Mn <sub>,</sub> Fe)PO <sub>4</sub> Solid Solution. Nano Letters, 2021, 21, 5091-5097.	9.1	9
24	Synergic modulation of over-stoichiometrical MnO2 and SiO2-coated particles on the energy storage properties of silver niobate-based ceramics. Ceramics International, 2021, 47, 19595-19604.	4.8	16
25	Simultaneous improved polarization and breakdown strength in Mn/W co-doped silver niobate ceramics. Journal of Materials Science, 2021, 56, 19155-19164.	3.7	8
26	Co-precipitation synthesis and electrochemical properties of NASICON-type Li1.3Al0.3Ti1.7(PO4)3 solid electrolytes. Journal of Materials Science: Materials in Electronics, 2021, 32, 24834-24844.	2.2	16
27	Uniform rotate hydrothermal synthesis of V6O13 nanosheets as cathode material for lithium-ion battery. Journal of Alloys and Compounds, 2021, 877, 160174.	5.5	19
28	Rational Design and Porosity of Porous Alumina Ceramic Membrane for Air Bearing. Membranes, 2021, 11, 872.	3.0	7
29	Enhanced discharged energy density of nanocomposites with dopamine@BaTiO <sub>3</sub> whiskers. Materials Technology, 2020, 35, 515-521.	3.0	2
30	Simultaneously improved dielectric constant and breakdown strength of PVDF/Nd-BaTiO3 fiber composite films via the surface modification and subtle filler content modulation. Composites Part A: Applied Science and Manufacturing, 2020, 128, 105675.	7.6	41
31	A promising composite solid electrolyte incorporating LLZO into PEO/PVDF matrix for all-solid-state lithium-ion batteries. Ionics, 2020, 26, 1101-1108.	2.4	50
32	Effects of the buffer layer on piezoelectric and ferroelectric properties of PMN-PT film-on-Ni foil composites. Journal of Materials Science: Materials in Electronics, 2020, 31, 677-683.	2.2	0
33	Processing and Enhanced Electrochemical Properties of Li7La3Zr2â^'xTixO12 Solid Electrolyte by Chemical Co-precipitation. Journal of Electronic Materials, 2020, 49, 4910-4915.	2.2	12
34	Interlayer-expanded MoS2 nanosheets/nitrogen-doped carbon as a high-performance anode for sodium-ion batteries. Journal of Alloys and Compounds, 2020, 838, 155541.	5.5	20
35	Hydrothermal synthesized AgNbO3 powders: Leading to greatly improved electric breakdown strength in ceramics. Journal of the European Ceramic Society, 2020, 40, 5589-5596.	5.7	21
36	The high energy density and efficiency of PVDF-based composites with double-shell Nd-BaTiO <sub>3</sub> particles as fillers. Functional Materials Letters, 2020, 13, 2051042.	1.2	6

#	Article	IF	CITATIONS
37	Large piezoelectricity and high transparency in fine-grained BaTiO3 ceramics. Applied Physics Letters, 2020, 116, .	3.3	10
38	A structural phase boundary due to oxygen octahedral tilt–untilt transition in Bi0.5Na0.5TiO3-based piezoelectric ceramics. Journal of Applied Physics, 2020, 127, .	2.5	8
39	Ferroelectric aging effects and large recoverable electrostrain in ceriaâ€doped BaTiO <sub>3</sub> ceramics. Journal of the American Ceramic Society, 2019, 102, 2611-2618.	3.8	7
40	High thermal stability of piezoelectric properties in tetragonal Pb(In1/3Nb2/3)O3-PbTiO3 single crystal. Journal of Applied Physics, 2019, 126, .	2.5	8
41	Effect of Ga-Bi Co-doped on Structural and Ionic Conductivity of Li7La3Zr2O12 Solid Electrolytes Derived from Sol–Gel Method. Journal of Electronic Materials, 2019, 48, 7762-7768.	2.2	5
42	Dielectric and energy storage properties of PVDF/Nd-BaTiO <sub>3</sub> @Al <sub>2</sub> O <sub>3</sub> composite films. Functional Materials Letters, 2019, 12, 1950034.	1.2	13
43	Formation of Ag3PO4/AgBr composites with Z-scheme configuration by an in situ strategy and their superior photocatalytic activity with excellent anti-photocorrosion performance. Journal of Materials Science: Materials in Electronics, 2019, 30, 11368-11377.	2.2	12
44	Controllable synthesis of 3D Fe <sub>3</sub> O <sub>4</sub> micro-cubes as anode materials for lithium ion batteries. CrystEngComm, 2019, 21, 5050-5058.	2.6	9
45	In-situ fabrication of MoO3 nanobelts decorated with MoO2 nanoparticles and their enhanced photocatalytic performance. Applied Surface Science, 2019, 480, 427-437.	6.1	61
46	Flexible polyvinylidene fluoride based nanocomposites with high and stable piezoelectric performance over a wide temperature range utilizing the strong multi-interface effect. Composites Science and Technology, 2019, 174, 33-41.	7.8	21
47	Photo-Fenton reaction and H2O2 enhanced photocatalytic activity of α-Fe2O3 nanoparticles obtained by a simple decomposition route. Journal of Alloys and Compounds, 2019, 771, 398-405.	5.5	52
48	Enhanced thermoelectric properties of nano-SiC dispersed NaCo <sub>2</sub> O <sub>4</sub> composites. Functional Materials Letters, 2019, 12, 1950009.	1.2	11
49	One-step fabrication of in situ carbon-coated NiCo2O4@C bilayered hybrid nanostructural arrays as free-standing anode for high-performance lithium-ion batteries. Electrochimica Acta, 2018, 273, 1-9.	5.2	39
50	Construction of novel BiOCl/MoS2 nanocomposites with Z-scheme structure for enhanced photocatalytic activity. Materials Letters, 2018, 218, 110-114.	2.6	28
51	Orientation-Dependent Lithium Miscibility Gap in LiFePO <sub>4</sub> . Chemistry of Materials, 2018, 30, 874-878.	6.7	33
52	High discharged energy density of polymer nanocomposites induced by Nd-doped BaTiO3 nanoparticles. Journal of Materiomics, 2018, 4, 44-50.	5.7	31
53	Effects of period number and sputtering time on optical properties of Si/Ge multilayer films deposited by magnetron sputtering. Journal of Materials Science: Materials in Electronics, 2018, 29, 1672-1679.	2.2	0
54	Green synthesis of high-performance LiFePO <sub>4</sub> nanocrystals in pure water. Green Chemistry, 2018, 20, 5215-5223.	9.0	25

#	Article	IF	CITATIONS
55	One-step and short-time synthesis of 3D NaV2O5 mesocrystal as anode materials of Na-Ion batteries. Journal of Power Sources, 2018, 395, 158-162.	7.8	12
56	Effect of the orientation on the ferroelectricity, dielectricity and magnetoelectric coupling in the bilayered Pb(Zr0.52Ti0.48)O3 film-on-CoFe2O4 bulk ceramic composites. Journal of Alloys and Compounds, 2018, 762, 574-578.	5.5	6
57	Textured Na x CoO2 Ceramics Sintered from Hydrothermal Platelet Nanocrystals: Growth Mechanism and Transport Properties. Journal of Electronic Materials, 2018, 47, 4070-4077.	2.2	2
58	Influence of the phase transformation in NaxCoO2 ceramics on thermoelectric properties. Ceramics International, 2018, 44, 17251-17257.	4.8	18
59	3D hierarchical porous sponge-like V2O5 micro/nano-structures for high-performance Li-ion batteries. Journal of Alloys and Compounds, 2018, 765, 901-906.	5.5	25
60	Effect of rolling temperature on the microstructure and electric properties of β-polyvinylidene fluoride films. Journal of Materials Science: Materials in Electronics, 2018, 29, 15957-15965.	2.2	11
61	Effects of annealing process and the additive on the electrical properties of chemical solution deposition derived 0.65Pb(Mg1/3Nb2/3)O3–0.35PbTiO3 thin films. Journal of Materials Science: Materials in Electronics, 2018, 29, 16997-17002.	2.2	3
62	Anisotropy electric and optical properties of PIMNT single crystal. Journal of Nanophotonics, 2018, 12, 1.	1.0	15
63	Combination of ultrafast dye-sensitized-assisted electron transfer process and novel Z-scheme system: AgBr nanoparticles interspersed MoO3 nanobelts for enhancing photocatalytic performance of RhB. Applied Catalysis B: Environmental, 2017, 206, 242-251.	20.2	164
64	Crystalline Structure, Defect Chemistry and Room Temperature Colossal Permittivity of Nd-doped Barium Titanate. Scientific Reports, 2017, 7, 42274.	3.3	89
65	Precursorâ€Directed Nucleation and Selfâ€Assembly Growth: From Hollow Microprisms to Nanoplatelets. ChemNanoMat, 2017, 3, 292-297.	2.8	3
66	Tree-like Li2MnO3@CNT hierarchical architecture assembled for remarkable anode material. Journal of Alloys and Compounds, 2017, 708, 531-537.	5.5	5
67	Effects of Mn doping on dielectric and ferroelectric characteristics of lead-free (K, Na, Li)NbO3 thin films grown by chemical solution deposition. Journal of Materials Science: Materials in Electronics, 2017, 28, 487-492.	2.2	3
68	Ultrathin Nanoribbons of in Situ Carbon-Coated V <sub>3</sub> O <sub>7</sub> ·H <sub>2</sub> O for High-Energy and Long-Life Li-Ion Batteries: Synthesis, Electrochemical Performance, and Charge–Discharge Behavior. ACS Applied Materials & Interfaces, 2017, 9, 17002-17012.	8.0	53
69	Hierarchical Porous Intercalationâ€Type V <sub>2</sub> O <sub>3</sub> as Highâ€Performance Anode Materials for Liâ€lon Batteries. Chemistry - A European Journal, 2017, 23, 7538-7544.	3.3	63
70	Ultrathin VO <sub>2</sub> nanosheets self-assembled into 3D micro/nano-structured hierarchical porous sponge-like micro-bundles for long-life and high-rate Li-ion batteries. Journal of Materials Chemistry A, 2017, 5, 8307-8316.	10.3	86
71	Flexible and robust N-doped carbon nanofiber film encapsulating uniformly silica nanoparticles: Free-standing long-life and low-cost electrodes for Li- and Na-Ion batteries. Electrochimica Acta, 2017, 235, 79-87.	5.2	40
72	Revealing the hydrothermal crystallization mechanism of ilmenite-type sodium niobate microplates: the roles of potassium ions. CrystEngComm, 2017, 19, 5966-5972.	2.6	6

#	Article	IF	CITATIONS
73	Hierarchical bilayered hybrid nanostructural arrays of NiCo <sub>2</sub> O <sub>4</sub> micro-urchins and nanowires as a free-standing electrode with high loading for high-performance lithium-ion batteries. Nanoscale, 2017, 9, 14979-14989.	5.6	35
74	Recent Progress in the Applications of Vanadiumâ€Based Oxides on Energy Storage: from Lowâ€Dimensional Nanomaterials Synthesis to 3D Micro/Nanoâ€Structures and Freeâ€Standing Electrodes Fabrication. Advanced Energy Materials, 2017, 7, 1700547.	19.5	151
75	Dielectric and energy storage performances of PVDF-based composites with colossal permittivitied Nd-doped BaTiO3 nanoparticles as the filler. AIP Advances, 2017, 7, .	1.3	24
76	Experimental study and electromechanical model analysis of the nonlinear deformation behavior of IPMC actuators. Acta Mechanica Sinica/Lixue Xuebao, 2017, 33, 382-393.	3.4	14
77	Elucidating the effects of high temperature mixing method under hydrothermal condition (HTMM) on grain refinements and assembling structures. Powder Technology, 2017, 305, 440-446.	4.2	0
78	The effect of LaNiO3 thickness on the magnetoelectric response of Pb(Zr0.52Ti0.48)O3 film-on-CoFe2O4 ceramic composites. Journal of Materials Science, 2017, 52, 541-549.	3.7	5
79	Low-temperature sintering and enhanced dielectric properties of alkali niobate ceramics prepared from solvothermally synthesized nanopowders. Ceramics International, 2017, 43, 1135-1144.	4.8	18
80	Citrate complexing sol–gel process of lead-free (K,Na)NbO <sub>3</sub> ferroelectric films. Modern Physics Letters B, 2016, 30, 1650157.	1.9	6
81	Electrochemical properties of Li 2 MnO 3 nanowires with polycrystalline and monocrystalline states. Journal of Alloys and Compounds, 2016, 686, 496-502.	5.5	13
82	A metastable cubic phase of sodium niobate nanoparticles stabilized by chemically bonded solvent molecules. Physical Chemistry Chemical Physics, 2016, 18, 33171-33179.	2.8	16
83	Effects of annealing temperature on structure and electrical properties of (Na, K)NbO3 thin films grown by RF magnetron sputtering deposition. Journal of Materials Science: Materials in Electronics, 2016, 27, 899-905.	2.2	9
84	Influence of Zr/Ti atomic ratio and seed layer on the magnetoelectric coupling of Pb(Zr x Ti 1â^'x )O 3 film-on-CoFe 2 O 4 bulk ceramic composites. Ceramics International, 2016, 42, 14431-14437.	4.8	7
85	Oxidation-Sulfidation Approach for Vertically Growing MoS <sub>2</sub> Nanofilms Catalysts on Molybdenum Foils as Efficient HER Catalysts. Journal of Physical Chemistry C, 2016, 120, 25843-25850.	3.1	56
86	Improved sintering activity and piezoelectric properties of PZT ceramics from hydrothermally synthesized powders with Pb excess. Journal of Materials Science: Materials in Electronics, 2016, 27, 8573-8579.	2.2	13
87	Enhanced Actuation Response of Nafion-Based Ionic Polymer Metal Composites by Doping BaTiO <sub>3</sub> Nanoparticles. Journal of Physical Chemistry C, 2016, 120, 12377-12384.	3.1	29
88	Effects of surfactant and reaction time on the formation and photocatalytic performance of Cu2S thin films grown in situ on Cu foil by hydrothermal method. Journal of Alloys and Compounds, 2016, 685, 266-271.	5.5	13
89	Non-isothermal crystallization behavior of polypropylene/zinc oxide composites. Science and Engineering of Composite Materials, 2016, 23, 505-510.	1.4	5
90	Bundle-like α′-NaV <sub>2</sub> O <sub>5</sub> mesocrystals: from synthesis, growth mechanism to analysis of Na-ion intercalation/deintercalation abilities. Nanoscale, 2016, 8, 1975-1985.	5.6	30

#	Article	IF	CITATIONS
91	MWCNTs-TiO2 core-shell nanoassemblies for fabrication of poly(vinylidene fluoride) based composites with high breakdown strength and discharged energy density. Journal of Polymer Research, 2016, 23, 1.	2.4	11
92	Crystal orientation dependent optical transmittance and band gap of Na0.5Bi0.5TiO3–BaTiO3 single crystals. Physica B: Condensed Matter, 2016, 483, 44-47.	2.7	32
93	Dramatically improved piezoelectric properties of poly(vinylidene fluoride) composites by incorporating aligned TiO2@MWCNTs. Composites Science and Technology, 2016, 123, 259-267.	7.8	61
94	Study on compositions and changes of SEI film of Li 2 MnO 3 positive material during the cycles. Catalysis Today, 2016, 274, 116-122.	4.4	16
95	Stabilized temperature-dependent dielectric properties of Dy-doped BaTiO 3 ceramics derived from sol-hydrothermally synthesized nanopowders. Ceramics International, 2016, 42, 3170-3176.	4.8	36
96	[100]-Oriented LiFePO <sub>4</sub> Nanoflakes toward High Rate Li-Ion Battery Cathode. Nano Letters, 2016, 16, 795-799.	9.1	81
97	Electro-mechanical performance of polyurethane dielectric elastomer flexible micro-actuator composite modified with titanium dioxide-graphene hybrid fillers. Materials and Design, 2016, 90, 1069-1076.	7.0	67
98	Hydrothermal synthesis of spindle-like architectures of terbium hydroxide. Journal of the Ceramic Society of Japan, 2015, 123, 672-676.	1.1	3
99	A general and simple method to synthesize well-crystallized nanostructured vanadium oxides for high performance Li-ion batteries. Journal of Materials Chemistry A, 2015, 3, 9385-9389.	10.3	42
100	Enhanced dielectric tunability of Ba x Sr1â^'x TiO3–MgO composite ceramics co-modified with CuO and MnO2. Journal of Materials Science: Materials in Electronics, 2015, 26, 2107-2112.	2.2	8
101	Solvothermal Synthesis and Formation Mechanism of Potassium Sodium Niobate Mesocrystals Under Low Alkaline Conditions. Journal of Nanoscience and Nanotechnology, 2015, 15, 4934-4940.	0.9	6
102	Effects of excess sulfur source on the formation and photocatalytic properties of flower-like MoS2 spheres by hydrothermal synthesis. Materials Letters, 2015, 144, 153-156.	2.6	64
103	Microwave-assisted sol–hydrothermal synthesis of tetragonal barium titanate nanoparticles with hollow morphologies. Journal of Materials Science: Materials in Electronics, 2015, 26, 1597-1601.	2.2	12
104	Achieving High Performance Electric Field Induced Strain: A Rational Design of Hyperbranched Aromatic Polyamide Functionalized Graphene–Polyurethane Dielectric Elastomer Composites. Journal of Physical Chemistry B, 2015, 119, 4521-4530.	2.6	46
105	Comparative investigations on dielectric, piezoelectric properties and humidity resistance of PZT–SKN and PZT–SNN ceramics. Journal of Materials Science: Materials in Electronics, 2015, 26, 2897-2904.	2.2	9
106	Insight into influence of conducting polymer functionalized graphene on electromechanical activity of polyurethane-based intelligent shape-changing composites. Journal of Materials Science: Materials in Electronics, 2015, 26, 3730-3738.	2.2	12
107	Modified Solvothermal Strategy for Straightforward Synthesis of Cubic NaNbO <sub>3</sub> Nanowires with Enhanced Photocatalytic H <sub>2</sub> Evolution. Journal of Physical Chemistry C, 2015, 119, 25956-25964.	3.1	48
108	Dielectric, mechanical and electro-stimulus response properties studies of polyurethane dielectric elastomer modified by carbon nanotube-graphene nanosheet hybrid fillers. Polymer Testing, 2015, 47, 4-11.	4.8	50

#	Article	IF	CITATIONS
109	Electrochemical properties of Li <sub>2</sub> MnO <sub>3</sub> nanocrystals synthesized using a hydrothermal method. RSC Advances, 2015, 5, 71088-71094.	3.6	27
110	Copper Phthalocyanine Oligomer Noncovalent Functionalized Graphene-Polyurethane Dielectric Elastomer Composites for Flexible Micro-Actuator. Soft Materials, 2015, 13, 210-218.	1.7	21
111	Low-temperature solid-state synthesis and optical properties of ZnO/CdS nanocomposites. Journal of Alloys and Compounds, 2015, 618, 67-72.	5.5	25
112	Solvothermal synthesis of BaTiO3 nanoparticles from K2Ti6O13 precursors. Research on Chemical Intermediates, 2015, 41, 4851-4859.	2.7	4
113	Ultra high permittivity and significantly enhanced electric field induced strain in PEDOT:PSS–RGO@PU intelligent shape-changing electro-active polymers. RSC Advances, 2014, 4, 64061-64067.	3.6	50
114	Oneâ€Step Surfactantâ€Free Hydrothermal Synthesis of Platelike Sodium Niobate Template Powders. Journal of the American Ceramic Society, 2014, 97, 3360-3362.	3.8	12
115	Optical properties of (1-x)Pb(Zn1/3Nb2/3)O3-xPbTiO3single crystals. , 2014, , .		0
116	The effect of processing conditions on the crystal structure and electroactive properties of poly(vinylidene fluoride)/ multi-walled carbon nanotubes nanocomposites. , 2014, , .		0
117	Poly(methyl methacrylate)-functionalized graphene/polyurethane dielectric elastomer composites with superior electric field induced strain. Materials Letters, 2014, 128, 19-22.	2.6	45
118	Lead-free (K, Na)NbO3 thin films derived from chemical solution deposition modified with EDTA. Journal of Materials Science: Materials in Electronics, 2014, 25, 1112-1116.	2.2	11
119	Phase transition, microstructure, and dielectric properties of Li/Ta/Sb co-doped (K, Na)NbO3 lead-free ceramics. Ceramics International, 2014, 40, 4389-4394.	4.8	24
120	Effect of temperature on the crystalline phase and dielectric and ferroelectric properties of poly(vinylidene fluoride) film. Journal of Intelligent Material Systems and Structures, 2014, 25, 858-864.	2.5	17
121	Thickness dependence of magnetoelectric response for composites of Pb(Zr0.52Ti0.48)O3 films on CoFe2O4 ceramic substrates. AIP Advances, 2014, 4, .	1.3	5
122	Rod-like NaNbO <sub>3</sub> : mechanisms for stable solvothermal synthesis, temperature-mediated phase transitions and morphological evolution. RSC Advances, 2014, 4, 15104-15110.	3.6	16
123	Morphological and orientational diversity of LiFePO <sub>4</sub> crystallites: remarkable reaction path dependence in hydrothermal/solvothermal syntheses. CrystEngComm, 2014, 16, 10112-10122.	2.6	23
124	Enhanced dielectric and ferroelectric properties induced by TiO2@MWCNTs nanoparticles in flexible poly(vinylidene fluoride) composites. Composites Part A: Applied Science and Manufacturing, 2014, 65, 125-134.	7.6	93
125	Enhanced piezoelectric properties of 0.55Pb(Ni1/3Nb2/3)O3-0.135PbZrO3- 0.315PbTiO3 ternary ceramics by optimizing sintering temperature. Journal of Electroceramics, 2014, 32, 234-239.	2.0	36
126	Enhanced electrical properties of multiwalled carbon nanotube/poly(vinylidenefluoride) films through a rolling process. Journal of Materials Science: Materials in Electronics, 2014, 25, 2126-2137.	2.2	15

#	Article	IF	CITATIONS
127	Investigation of phase diagram and electrical properties of xPb(Mg1/3Nb2/3)O3–(1Ââ^Âx)Pb(Zr0.4Ti0.6)O3 ceramics. Journal of Materials Science: Materials in Electronics, 2014, 25, 3003-3009.	2.2	14
128	Enhanced electromagnetic wave absorption properties of polyaniline-coated Fe3O4/reduced graphene oxide nanocomposites. Journal of Materials Science: Materials in Electronics, 2014, 25, 3664-3673.	2.2	53
129	High-temperature-mixing hydrothermal synthesis of ZnO nanocrystals with wide growth window. Current Applied Physics, 2014, 14, 359-365.	2.4	16
130	Microstructure and piezoelectric properties of K5.70Li4.07Nb10.23O30-added K0.5Na0.5NbO3 ceramics. Journal of Advanced Ceramics, 2014, 3, 147-154.	17.4	4
131	Fabrication of BaTiO3 nanoparticles and its formation mechanism using the high temperature mixing method under hydrothermal conditions. Advanced Powder Technology, 2014, 25, 853-858.	4.1	19
132	Wavelength dependence of refractive index in lead-free Na0.5Bi0.5TiO3–BaTiO3 single crystals. Optical Materials, 2014, 36, 2023-2025.	3.6	26
133	Hydrothermally synthesized barium titanate nanostructures from K2Ti4O9 precursors: Morphology evolution and its growth mechanism. Materials Research Bulletin, 2014, 57, 162-169.	5.2	30
134	Influence of solvothermal treatment time on oxidation of carbon/carbon composites containing ZrB2 micro-particles. Ceramics International, 2014, 40, 13529-13535.	4.8	8
135	Low-Temperature Sintering of (K0.5Na0.5)NbO3 Piezoelectric Ceramics. Journal of Inorganic and Organometallic Polymers and Materials, 2013, 23, 463-466.	3.7	3
136	Influence of annealing temperature on the structural and optical properties of highly-oriented Al and Er co-doped ZnO films. Journal of Materials Science: Materials in Electronics, 2013, 24, 3868-3874.	2.2	3
137	Sol-solvothermal synthesis and characterization of fine lead zirconate titanate particles. Journal of Materials Science: Materials in Electronics, 2013, 24, 2264-2270.	2.2	4
138	Preparation and dielectric properties of a polyurethane elastomer filled with resol-derived ordered mesoporous carbon. Journal of Materials Science: Materials in Electronics, 2013, 24, 2013-2018.	2.2	6
139	Electrical and optical properties of Nd <sup>3+</sup> -doped Na <sub>0.5</sub> Bi <sub>0.5</sub> TiO <sub>3</sub> ferroelectric single crystal. Journal Physics D: Applied Physics, 2013, 46, 245104.	2.8	67
140	Microstructure, temperature stability and electrical properties of ZnO-modified Pb(Ni1/3Nb2/3)O3–Pb(Fe1/2Nb1/2)O3–Pb(Zr0.3Ti0.7)O3 piezoelectric ceramics. Ceramics International, 2013, 39, 9385-9390.	4.8	16
141	Preparation and characterization of monodispersed BaTiO3 nanocrystals by sol–hydrothemal method. Journal of Crystal Growth, 2013, 363, 300-307.	1.5	42
142	Influence of sintering temperature on electrical properties of (K0.4425Na0.52Li0.0375)(Nb0.8825Sb0.07Ta0.0475)O3 ceramics without phase transition induced by sintering temperature. Journal of Advanced Ceramics, 2013, 2, 353-359.	17.4	10
143	Sol-hydrothermal synthesis and characterization of lead zirconate titanate fine particles. Advanced Powder Technology, 2013, 24, 212-217.	4.1	14

Phase transition behavior and temperature-stable piezoelectric properties of new quaternary (K,) Tj ETQq0 0 0 rgBT  $\frac{1}{4.8}$  Verlock 10 Tf 50 6

#	Article	IF	CITATIONS
145	Origin of the low piezoelectric coefficient of metal core 0.3Pb(Zn1/3Nb2/3)O3–0.7Pb(Zr,Ti)O3 piezoelectric fibers. Journal of Alloys and Compounds, 2013, 581, 468-471.	5.5	3
146	Ultra-long VO2 (A) nanorods using the high-temperature mixing method under hydrothermal conditions: synthesis, evolution and thermochromic properties. CrystEngComm, 2013, 15, 2753.	2.6	58
147	Synthesis and Characterization of K(Ta <sub><i>x</i></sub> Nb <sub>1â^²<i>x</i></sub> )O <sub>3</sub> Particles by High Temperature Mixing Method Under Hydrothermal and Solvothermal Conditions. Journal of Nanoscience and Nanotechnology, 2013, 13, 1317-1322.	0.9	1
148	Fabrication and characterization of relaxor-ferroelectric 0.55Pb(Ni <sub>1/3</sub> Nb <sub>2/3</sub> )O <sub>3</sub> -0.45Pb(Zr <sub>0.3</sub> Ti <sub>0.7</sub> )O <sub>aceramics with sintering aid. , 2012, , .</sub>	ub>3 <td>0&gt;0</td>	0>0
149	Composition and orientation dependence of high electric-field-induced strain in Pb(In1/2Nb1/2)O3–Pb(Mg1/3Nb2/3)O3–PbTiO3 single crystals. Journal of Applied Physics, 2012, 112, 12610	)2 <sup>2.5</sup>	23
150	Temperature stability and fabrication of Pb(Zn1/3Nb2/3)O3–Pb(Zr,Ti)O3 fibers with Pt core. Journal of Intelligent Material Systems and Structures, 2012, 23, 1735-1740.	2.5	5
151	Orientation effects on the bandgap and dispersion behavior of 0.91Pb(Zn <sub>1/3</sub> Nb <sub>2/3</sub> )O <sub>3</sub> -0.09PbTiO <sub>3</sub> 3Chinese Physics B, 2012, 21, 054207.	1.4	25
152	Synthesis and Characterization of (K0.5Na0.5)NbO3Piezoelectric Ceramics Prepared Using K5.70Li4.07Nb10.23O30as a New Sintering Aid. Ferroelectrics, 2012, 432, 73-80.	0.6	2
153	Electrical properties and sensing ability of novel piezoelectric ceramic fibers with Pt core. Proceedings of SPIE, 2012, , .	0.8	0
154	Characterization and synthesis of KTa0.1Nb0.9O3 particles via high temperature mixing method under hydrothermal conditions. Advanced Powder Technology, 2012, 23, 558-561.	4.1	6
155	Hydrothermal synthesis of sodium niobate with controllable shape and structure. CrystEngComm, 2012, 14, 411-416.	2.6	38
156	The effects of ZnO layer and annealing temperature on the structure, optical and film–substrate cohesion properties of SiGe thin films prepared by radio frequency magnetron sputtering. Applied Surface Science, 2012, 259, 393-398.	6.1	8
157	Effect of CuO on dielectric and piezoelectric properties of (K0.4425Na0.52Li0.0375)(Nb0.87Ta0.06Sb0.07)O3 ceramics. Journal of Alloys and Compounds, 2012, 515, 128-133.	5.5	19
158	Synthesis and photoluminescence properties of single-crystal ZnO hexagonal pyramids by PEG400-assisted thermal decomposition route. Transactions of Nonferrous Metals Society of China, 2012, 22, 2459-2464.	4.2	4
159	Synthesis of potassium sodium niobate powders using an EDTA/citrate complexing sol–gel method. Particuology, 2012, 10, 777-782.	3.6	27
160	Effective electroâ€optic coefficient of (1– <i>x</i> )Pb(Zn <sub>1/3</sub> Nb <sub>2/3</sub> )O <sub>3</sub> – <i>x</i> PbTiO <sub>3</sub> single crystals. Crystal Research and Technology, 2012, 47, 610-614.	1.3	31
161	Tantalum influence on electrical properties of lead-free (K0.4425Na0.52Li0.0375)(Nb0.93â^'x Ta x Sb0.07) O3 piezoelectric ceramics. Journal of Materials Science: Materials in Electronics, 2012, 23, 846-850.	2.2	13
162	Effect of ZnO on the microstructure and electrical properties of (K0.5Na0.5)NbO3 lead-free piezoelectric ceramics. Journal of Materials Science: Materials in Electronics, 2012, 23, 1083-1086.	2.2	25

#	Article	IF	CITATIONS
163	Influence of sintering temperature on microstructure and electric properties of CuO doped alkaline niobate-based lead-free ceramics. Journal of Materials Science: Materials in Electronics, 2012, 23, 1455-1461.	2.2	10
164	Preparation and optical properties of high-quality oriented of Al and Er co-doped ZnO thin films. Journal of Sol-Gel Science and Technology, 2012, 63, 95-102.	2.4	11
165	A piezoelectric tracked vehicle with potential application to planetary exploration. Science Bulletin, 2012, 57, 1339-1342.	1.7	10
166	Effects of Sb content on electrical properties of lead-free piezoelectric (K0.4425Na0.52Li0.0375) (Nb0.9625â~'xSbxTa0.0375)O3 ceramics. Ceramics International, 2012, 38, 1249-1254.	4.8	9
167	Synthesis of (K, Na) (Nb, Ta)O3 lead-free piezoelectric ceramic powders by high temperature mixing method under hydrothermal conditions. Ceramics International, 2012, 38, 1807-1813.	4.8	33
168	(K, Na)NbO3-based lead-free piezoelectric ceramics manufactured by two-step sintering. Ceramics International, 2012, 38, 2521-2527.	4.8	39
169	Multi-modal vibration control using amended disturbance observer compensation. IET Control Theory and Applications, 2012, 6, 72.	2.1	24
170	Sol–gel synthesis, characterization and microwave absorbing properties of nano sized spherical particles of La0.8Sr0.2Mn0.8Fe0.2O3. Materials Research Bulletin, 2012, 47, 1961-1967.	5.2	14
171	Effects of Fe2O3 doping on the microstructure and piezoelectric properties of 0.55Pb(Ni1/3Nb2/3)O3–0.45Pb(Zr0.3Ti0.7)O3 ceramics. Materials Letters, 2012, 66, 153-155.	2.6	35
172	Sol-gel processing and characterization of potassium niobate nano-powders by an EDTA/citrate complexing method. Solid State Sciences, 2012, 14, 655-660.	3.2	9
173	PZT Powders Synthesized by Hydrothermal Method. Wuji Cailiao Xuebao/Journal of Inorganic Materials, 2012, 27, 507-512.	1.3	2
174	Effects of the Calcining Temperature on the Piezoelectric and Dielectric Properties of 0.55PNN-0.45PZT Ceramics. Ferroelectrics, 2011, 425, 90-97.	0.6	10
175	Linear electro-optic properties of orthorhombic PZN-8%PT single crystal. IEEE Transactions on Ultrasonics, Ferroelectrics, and Frequency Control, 2011, 58, 1118-1121.	3.0	5
176	Full tensorial elastic, piezoelectric, and dielectric properties characterization of [011]-poled PZN-9%PT single crystal. IEEE Transactions on Ultrasonics, Ferroelectrics, and Frequency Control, 2011, 58, 1127-1130.	3.0	32
177	Morphotropic Phase Boundary of Sodium–Potassium Niobate Leadâ€Free Piezoelectric Ceramics. Journal of the American Ceramic Society, 2011, 94, 796-801.	3.8	9
178	Piezoelectric vibration control for all-clamped panel using DOB-based optimal control. Mechatronics, 2011, 21, 1213-1221.	3.3	37
179	Fabrication of 0.655Pb(Mg1/3Nb2/3)O3-0.345PbTiO3 functionally graded piezoelectric actuator by tape-casting. Journal of Electroceramics, 2011, 27, 197-202.	2.0	9
180	Study on the sintering mechanism of KNN-based lead-free piezoelectric ceramics. Journal of Materials Science, 2011, 46, 2345-2349.	3.7	19

#	Article	IF	CITATIONS
181	Influence of sintering temperature on piezoelectric properties of (K0.4425Na0.52Li0.0375)(Nb0.8925Sb0.07Ta0.0375)O3 lead-free piezoelectric ceramics. Journal of Materials Science: Materials in Electronics, 2011, 22, 1783-1787.	2.2	18
182	Synthesis of (K,Na)NbO3 particles by traditional hydrothermal method and high-temperature mixing method under hydrothermal–solvothermal conditions. Research on Chemical Intermediates, 2011, 37, 185-193.	2.7	4
183	Control design for arbitrary complex nonlinear discrete-time systems based on direct NNMRAC strategy. Journal of Process Control, 2011, 21, 103-110.	3.3	11
184	Composition dependence of dispersion and bandgap properties in PZN- <i>x</i> PT single crystals. Journal of Applied Physics, 2011, 110, .	2.5	38
185	Solgel Self-Combustion Synthesis and Characterization of La <sub>0.8</sub> Sr <sub>0.2</sub> Mn <sub>0.8</sub> Fe <sub>0.2</sub> O <sub>3</sub> . Advanced Materials Research, 2011, 326, 131-138.	0.3	3
186	Low Temperature Sintering and Properties of (K <sub>0.5</sub> Na <sub>0.5</sub> )NbO <sub>3</sub> Piezoelectric Ceramics. Japanese Journal of Applied Physics, 2011, 50, 110203.	1.5	6
187	Tracking control of piezoelectric actuator system using inverse hysteresis model. International Journal of Applied Electromagnetics and Mechanics, 2010, 33, 1555-1564.	0.6	13
188	Isopropanol-assisted hydrothermal synthesis of (K, Na)NbO3 piezoelectric ceramic powders. Journal of Materials Science, 2010, 45, 3311-3317.	3.7	16
189	Coprecipitation-assisted hydrothermal synthesis of PLZT hollow nanospheres. Materials Research Bulletin, 2010, 45, 969-973.	5.2	6
190	Synthesis of (K, Na)NbO3 particles by high temperature mixing method under hydrothermal conditions. Materials Letters, 2010, 64, 77-79.	2.6	22
191	A low-power circuit for piezoelectric vibration control by synchronized switching on voltage sources. Sensors and Actuators A: Physical, 2010, 161, 245-255.	4.1	60
192	Two-mode vibration control of a beam using nonlinear synchronized switching damping based on the maximization of converted energy. Journal of Sound and Vibration, 2010, 329, 2751-2767.	3.9	54
193	Crystallographic study of lead-substituted hydroxyapatite synthesized by high-temperature mixing method under hydrothermal conditions. Inorganica Chimica Acta, 2010, 363, 1785-1790.	2.4	19
194	Phase evolution of (K, Na)NbO3 powder prepared by high temperature mixing under hydrothermal conditions. Particuology, 2010, 8, 477-481.	3.6	12
195	Metal core piezoelectric ceramic fiber rosettes for acousto-ultrasonic source localization in plate structures. International Journal of Applied Electromagnetics and Mechanics, 2010, 33, 865-873.	0.6	15
196	Lamb wave sensing with metal-core piezoelectric fiber for structural health monitoring. , 2010, , .		0
197	RESPONSE OF METAL CORE PIEZOELECTRIC FIBERS TO UNSTEADY AIRFLOWS. Modern Physics Letters B, 2010, 24, 1453-1456.	1.9	15
	Ferroelectric and Piezoelectric Properties of		

Pb(Ni<sub>1/3</sub>Nb<sub>2/3</sub>)<sub>0.5</sub>(Ti<sub>0.7</sub>Zr<sub>0.3</sub>)<sub>0.5</sub>O@sub>3</sub>Ceram Fabricated by Tape-Casting Process. Ferroelectrics, 2010, 396, 90-97.

#	Article	IF	CITATIONS
199	Metal-Core Piezoelectric Fibers for the Detection of Lamb Waves. , 2010, , .		0
200	Effects of Sb-doping on the formation of (K, Na)(Nb, Sb)O3 solid solution under hydrothermal conditions. Journal of Alloys and Compounds, 2010, 493, 186-191.	5.5	21
201	Enhanced synchronized switch harvesting: a new energy harvesting scheme for efficient energy extraction. Smart Materials and Structures, 2010, 19, 115017.	3.5	84
202	Hydrothermal Solvothermal Synthesis of (K, Na)NbO <sub>3</sub> Lead-free Piezo-electric Ceramics and Its Properties. Wuji Cailiao Xuebao/Journal of Inorganic Materials, 2010, 25, 1159-1163.	1.3	3
203	Vibration Control of a Composite Beam Using Self-sensing Semi-active Approach. Chinese Journal of Mechanical Engineering (English Edition), 2010, 23, 663.	3.7	10
204	An Improved System of Active Noise Isolation Using a Self-sensing Actuator and Neural Network. JVC/Journal of Vibration and Control, 2009, 15, 1853-1873.	2.6	11
205	Two-Step Sintering of the Pure K <sub>0.5</sub> Na <sub>0.5</sub> NbO <sub>3</sub> Lead-Free Piezoceramics and Its Piezoelectric Properties. Ferroelectrics, 2009, 392, 120-126.	0.6	32
206	FABRICATION AND PERFORMANCE OF HIGH TEMPERATURE STYLE FUNCTIONALLY GRADED PIEZOELECTRIC BENDING ACTUATORS. Modern Physics Letters B, 2009, 23, 433-436.	1.9	5
207	Modeling and simulation of piezoelectric composite diaphragms for energy harvesting. International Journal of Applied Electromagnetics and Mechanics, 2009, 30, 95-106.	0.6	28
208	Fabrication of lead-free barium titanate piezoelectric ceramics from barium titanate powders with different particle sizes synthesized by hydrothermal method. International Journal of Applied Electromagnetics and Mechanics, 2009, 31, 9-16.	0.6	1
209	A semi-passive vibration damping system powered by harvested energy. International Journal of Applied Electromagnetics and Mechanics, 2009, 31, 219-233.	0.6	10
210	The constitutive equations of half coated metal core piezoelectric fiber. International Journal of Applied Electromagnetics and Mechanics, 2009, 29, 47-64.	0.6	16
211	Morphology variation of cadmium hydroxyapatite synthesized by high temperature mixing method under hydrothermal conditions. Materials Chemistry and Physics, 2009, 113, 239-243.	4.0	32
212	Synthesis and crystallographic study of Pb–Sr hydroxyapatite solid solutions by high temperature mixing method under hydrothermal conditions. Materials Research Bulletin, 2009, 44, 1392-1396.	5.2	25
213	Novel Fe/glass composite adsorbent for As(V) removal. Journal of Environmental Sciences, 2009, 21, 434-439.	6.1	6
214	Effect of washing of barium titanate powders synthesized by hydrothermal method on their sinterability and piezoelectric properties. Ceramics International, 2009, 35, 1947-1951.	4.8	17
215	Comparison between four piezoelectric energy harvesting circuits. Frontiers of Mechanical Engineering in China, 2009, 4, 153-159.	0.4	72
216	Microstructure and electrical properties of NaNbO3-BaTiO3 lead-free piezoelectric ceramics. Frontiers of Mechanical Engineering in China, 2009, 4, 345.	0.4	0

#	Article	IF	CITATIONS
217	Semi-active vibration control using piezoelectric actuators in smart structures. Frontiers of Mechanical Engineering in China, 2009, 4, 242.	0.4	24
218	Semi-active Vibration Control of a Composite Beam by Adaptive Synchronized Switching on Voltage Sources Based on LMS Algorithm. Journal of Intelligent Material Systems and Structures, 2009, 20, 939-947.	2.5	53
219	Semi-active Vibration Control of a Composite Beam using an Adaptive SSDV Approach. Journal of Intelligent Material Systems and Structures, 2009, 20, 401-412.	2.5	56
220	Multi-modal vibration control using a synchronized switch based on a displacement switching threshold. Smart Materials and Structures, 2009, 18, 035016.	3.5	31
221	Piezoelectric devices and their application in smart structures. , 2008, , .		1
222	Vibration control of a composite beam by an adaptive semi-active method based on LMS algorithm. , 2008, , .		2
223	The vibration sensor of metal core piezoelectric fiber. , 2008, , .		0
224	Stable resonance characteristics in CuO-modified lead-free 0.94(K <inf>0.5</inf> Na <inf>0.5</inf> )NbO <inf>3</inf> -0.06LiNbO <inf>3&amp;l ceramics sintered at optimal temperature. , 2008, , .</inf>	;/inf>	1
225	Research on the response of piezoelectric ceramic fibers with metal core to Lamb waves. , 2008, , .		0
226	Hydrothermal synthesis of (K,Na)(Nb,Ta)O 3 powder for fabrication of lead-free piezoelectric ceramics. Proceedings of SPIE, 2007, 6423, 33.	0.8	0
227	Hydrothermal Synthesis and Crystallographic Study of Sr-Pb Hydroxyapatite Solid Solutions. Journal of the Ceramic Society of Japan, 2007, 115, 873-876.	1.1	7
228	Preparation of calcium doped LaCrO3 fine powders by hydrothermal method and its sintering. Journal of the European Ceramic Society, 2006, 26, 81-88.	5.7	42
229	Preferential occupancy of metal ions in the hydroxyapatite solid solutions synthesized by hydrothermal method. Journal of the European Ceramic Society, 2006, 26, 509-513.	5.7	107
230	Preparation of Hydroxyapatite Ceramics by Hydrothermal Hot-Pressing Technique. Key Engineering Materials, 2006, 309-311, 57-60.	0.4	5
231	HYDROTHERMAL PREPARATION OF HYDROXYAPATITE SOLID SOLUTIONS WITH VARIOUS METAL IONS. Phosphorus Research Bulletin, 2005, 19, 99-105.	0.6	0
232	Hydrothermal synthesis and sintering of lanthanum chromite powders doped with calcium. Solid State Ionics, 2004, 172, 389-392.	2.7	27
233	Hydrothermal synthesis and morphology variation of cadmium hydroxyapatite. Journal of Solid State Chemistry, 2004, 177, 4379-4385.	2.9	26
234	HYDROTHERMAL SYNTHESIS AND CRYSTALLOGRAPHIC STUDY OF Ca-Sr HYDROXYAPATITE SOLID SOLUTIONS. Phosphorus Research Bulletin, 2004, 17, 215-220.	0.6	8

#	Article	IF	CITATIONS
235	DEVELOPMENT OF LOW TEMPERATURE SINTERING OF HYDROXYAPATITE CERAMICS USING HYDROTHERMAL HOT-PRESSING METHOD. Phosphorus Research Bulletin, 2004, 17, 231-234.	0.6	3
236	Reduced graphene oxide modified V6O13 nanostructure hybrids with high pseudocapacitance contribution as cathode for highâ€rate lithium storage. ChemElectroChem, 0, , .	3.4	1